

Discrete Time Credit-Based Shaping for Time-Sensitive Applications in 5G/6G Networks

Anudeep Karnam, Kishor C. Joshi, Jobish John, George Exarchakos, Sonia Heemstra de Groot, Ignas Niemegeers
Center for Wireless Technology Eindhoven, Eindhoven University of Technology, The Netherlands.

Abstract—Future wireless networks must deliver deterministic end-to-end delays for workloads such as smart-factory control loops. On Ethernet these guarantees are delivered by the set of tools within IEEE 802.1 time sensitive networking (TSN) standards. Credit-based shaper (CBS) is one such tool which enforces bounded latency. Directly porting CBS to 5G/6G New Radio (NR) is non-trivial because NR schedules traffic in discrete-time, modulation-dependent resource allocation, whereas CBS assumes a continuous, fixed-rate link. Existing TSN-over-5G translators map Ethernet priorities to 5G quality of service (QoS) identifiers but leave the radio scheduler unchanged, so deterministic delay is lost within the radio access network (RAN). To address this challenge, we propose a novel slot-native approach that adapts CBS to operate natively in discrete NR slots. We first propose a per-slot credit formulation for each user-equipment (UE) queue that debits credit by the granted transport block size (TBS); we call this discrete-time CBS (CBS-DT). Recognizing that debiting the full TBS can unduly penalize transmissions that actually use only part of their grant, we then introduce and analyze CBS with Partial Usage (CBS-PU). CBS-PU scales the credit debit in proportion to the actual bytes dequeued from the downlink queue. The resulting CBS-PU algorithm is shown to maintain bounded credit, preserve long-term rate reservations, and guarantees worst-case delay performance no worse than CBS-DT. Simulation results show that slot-level credit gating—particularly CBS-PU—enables NR to export TSN class QoS while maximizing resource utilization.

I. INTRODUCTION

Beyond-5G (B5G) and 6G networks are expected to accommodate diverse quality of service (QoS) requirements [1]. Emerging Industry 5.0 scenarios—smart factories, and real-time motion control—tighten these requirements, including end-to-end latencies below 1ms and microsecond-level jitter, with reliability exceeding 99.999% [2]. Wired Ethernet already achieves such determinism through the IEEE Time-Sensitive Networking (TSN) tool-set, which combines per-flow traffic shaping with schedule-driven queuing to guarantee hard deadlines [3]. Replicating such stringent guarantees over the inherently stochastic wireless air interface is highly challenging [4].

One promising approach draws inspiration from Ethernet networks, where IEEE 802.1Qav’s [5] credit-based shaper (CBS) achieves deterministic performance. As long as the aggregate reserved rate is strictly below the link capacity, each flow’s queuing delay is deterministically bounded [6]. Adapting this credit logic for wireless networks would therefore extend predictable, bounded latency to high-priority traffic, while still ensuring that lower-priority flows cannot exceed their allocated share.

This work has been submitted to the IEEE for possible publication. Copyright may be transferred without notice.

Prior work adapting CBS to wireless networks includes the wireless credit-based shaper algorithm (WCBSA) proposed for IEEE 802.11aa [7] equipping each 802.11 station (STA) with two internal queues. Credit accrual is frozen during contention phases and resumes only after the medium is won. The design assumes (i) a fixed rate, error-free 802.11a physical (PHY) layer, and (ii) fair medium-access conditions. These assumptions are invalid in 5G new radio (NR), where the base station issues dynamic, unequal grants, bit rates vary with modulation coding schemes (MCS), and channel access is centrally scheduled in discrete slot intervals rather than through decentralized contention-based medium access. Thus, WCBSA is unsuitable for per-UE credit shaping in NR. Current proposals for TSN-over-5G [8] use TSN translators (TTs) at the user equipment (UE) and at the user plane function (UPF) in the core network, and consider the 5G network as a logical bridge within the TSN framework [9]. Specifically, in such an architecture the device side TT (DS-TT) and network-side TT (NW-TT) act as the Ethernet-to-5G bridge ports mapping TSN information to appropriate 5G parameters such as QoS Flow Identifier (QFI) or 5G QoS Identifier (5QI) (and vice-versa) [10]. While such translators enable end-to-end TSN connectivity, the resource management *inside* the radio-access network (RAN) still relies on the 5G framework.

Hence, even when a 5G RAN is augmented with TTs that map Ethernet priorities into 5QI/QFI values, the underlying resource-allocation logic within the RAN itself remains the legacy grant scheduler [11]. Thus, while end-to-end TSN systems can continuously track credit or enforce per-flow rate reservations, the standard NR scheduler neither tracks credit continuously nor ensures per-UE rate reservations at the slot level. What is still missing is a slot-native credit algorithm that resides inside the gNB itself, debits credit every time a grant is issued. This paper fills this gap by proposing an explicit discrete-time formulation for credit evolution and embedding it directly into the NR MAC. The result is a per-UE CBS variant for operation within the time-slotted scheduling environment of 5G-NR. The major contributions of the paper are as follows:

- 1) We propose a discrete-time slot-native CBS adaptation, termed as CBS-DT, where the per-slot credit debit is directly coupled to the granted transport block size (TBS). We further study the stability properties (credit boundedness, deficit recovery) introduced by channel quality and resource allocation.
- 2) We identify the inefficiency of TBS-based debiting when

grants are partially utilized in CBS-DT variant. To overcome this we propose CBS with partial usage (CBS-PU), where the credit debit is scaled proportionally to the actual bytes transmitted, mitigating excessive credit depletion.

- 3) We provide a comparative performance evaluation of CBS variants focusing on metrics like end-to-end latency differentiation across priorities and resource utilization efficiency under varying load.

The remainder of this paper is organized as follows. Section II outlines TSN CBS and its limitations in 5G NR. Section III details our system model. Section IV formalizes our CBS-DT adaptation, while Section V introduces the CBS-PU mechanism. Simulation results validating both CBS adaptations are presented in Section VI, followed by conclusions in Section VII.

II. BACKGROUND: CREDIT-BASED SHAPING IN TIME-SENSITIVE NETWORKING

CBS [5] offers per-class bandwidth reservation and contributes to predictable latency by ensuring bounded queuing delays on shared links, working in conjunction with other mechanisms like the time aware shaper (TAS) for tight delay bounds in Ethernet. Each prioritized traffic class is assigned a dedicated queue, indexed by p . Each queue maintains a continuous-time credit, $C_p(t)$, and packets are transmitted only when $C_p(t) \geq 0$ [12]. Among queues that are both backlogged (i.e., have data to send) and meet this eligibility condition of having non-negative credit, CBS strictly prioritizes the highest priority queue for transmission, allowing preferential treatment and deterministic latency control for critical traffic.

A. Credit Dynamics: *IdleSlope* and *SendSlope*

The credit $C_p(t)$ continuously evolves over t based on two CBS parameters and the queue's operational state:

- 1) **idleSlope** (α_p^+): The rate (bits/s or bytes/s) at which credit *accumulates* when queue p is eligible but not transmitting (due to being empty or blocked by higher priority). α_p^+ represents the bandwidth share *reserved* for traffic class p over time.
- 2) **sendSlope** (α_p^-): The rate at which credit is *consumed* while queue p is transmitting. It is formally defined as: $\alpha_p^- = \alpha_p^+ - R_{\text{link}}$, where R_{link} is the physical link rate, making α_p^- negative, reflecting credit consumption during transmission.

If queue p is idle (either no pending load and $C_p(t) \geq 0$, or $C_p(t) < 0$ and not transmitting, or pending load but blocked by other traffic), its credit increases. For any two time instances t_1, t_2 and $t_2 > t_1$ the credit updates as [13]:

$$C_p(t_2) = C_p(t_1) + \alpha_p^+ \cdot (t_2 - t_1) \quad (1)$$

If queue p is actively transmitting:

$$C_p(t_2) = C_p(t_1) - \alpha_p^- \cdot (t_2 - t_1) \quad (2)$$

The credit is reset to zero if the queue becomes empty and $C_p(t) \geq 0$ (Eq. 3.18 in [13]).

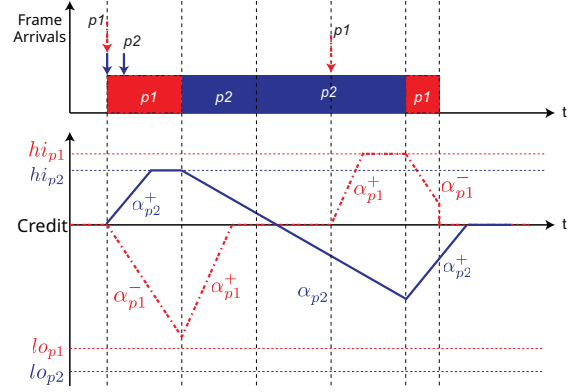


Fig. 1: CBS example with priorities p_1 (high) and p_2 (low)

B. Credit Limits: *hiCredit* and *loCredit*

To prevent unbounded credit accumulation or deficit, CBS employs upper and lower bounds on $C_p(t)$:

- 1) **hiCredit** (hi_p): The maximum positive credit value queue p is allowed to accumulate. hi_p limits the maximum burst size that the queue p can transmit immediately following an idle period.
- 2) **loCredit** (lo_p): The minimum credit value queue p can reach, ensuring that even after transmitting a maximum-sized frame, the queue's credit deficit is bounded. This, in turn, bounds the maximum time required for the queue to recover positive credit solely through the accumulation via *idleSlope*. The credit is clamped within $[lo_p, hi_p]$.

Fig. 1 illustrates CBS with two classes. A frame starts only when its credit is non-negative and it has frames to transmit; p_1 (high priority) is chosen over p_2 if both qualify. Credit accumulates at the reserved rate α_p^+ when idle and is consumed at α_p^- during transmission and are clamped at $[lo_{p1}, hi_{p1}]$ and $[lo_{p2}, hi_{p2}]$ respectively. Therefore, by consumption and accumulation of credits prevents a single high priority queue from monopolizing the link indefinitely.

C. Why Does Classical CBS Fail in a 5G NR Scheduler?

The key assumptions in IEEE 802.1Qav CBS are: (i) *continuous time* credit evolution; (ii) a *single, fixed link rate* R_{link} ; and (iii) shaping a single queue at a particular time instant that outputs frames without needing complex resource allocation (RA) procedures. On the other hand, 5G NR presents a fundamentally different operational context, invalidating these assumptions, posing significant challenges for implementing CBS within the RAN.

1) *Slot-quantized time*: NR operates in discrete slots (T_{slot}), requiring discrete credit updates.

2) *Grant-dependent rate*: 5G service rates are grant-dependent, unlike the fixed link rate in CBS.

3) *Multi-user multiplexing*: A wired port serves one frame at a time; NR can schedule multiple UEs/flows concurrently.

4) *Feedback-coupled retransmissions*: Automatic repeat request (ARQ) and Hybrid-ARQ (HARQ) can force a protocol data unit (PDU) to be transmitted multiple times; classical CBS

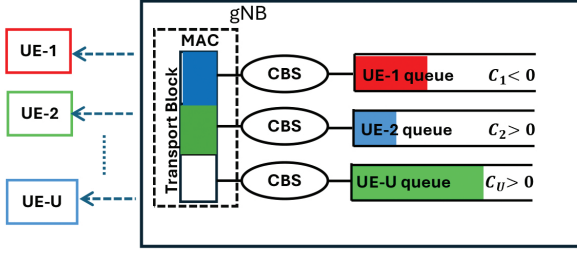


Fig. 2: Per-UE CBS gating in 5G-NR gNB downlink

is designed for reliable wires and has no such mechanisms. Consequently, these departures from the classical CBS—specifically, discrete operational timeline, highly dynamic service rates tied to scheduling grants and channel quality, concurrent servicing of multiple users, and the complexities introduced by wireless MAC/PHY feedback loops—invalidate key assumptions, making direct porting non-trivial. Effectively applying credit-based shaping within the 5G NR RAN mandates a rethinking of the mechanism, particularly requiring a discrete-time credit evolution logic accounting for the variable service provided in each transmission time interval (TTI).

III. SYSTEM MODEL

We consider a single-cell 5G NR downlink¹ that operates in *frequency-division duplex* (FDD). A gNB serves a finite set of static UEs $\mathcal{U} \triangleq \{1, \dots, U\}$, as shown in Fig.2, with the 3GPP Urban Macro (UMa) channel model [14]. Uplink control signaling—buffer status reports (BSRs) and channel quality indicator (CQI)—is assumed timely and error-free.

Traffic and QoS hierarchy: Each UE carries exactly one QoS flow and is assigned a priority $p : \mathcal{U} \rightarrow \mathcal{P} = \{p_1, \dots, p_P\}$, where $p(u) = p_1$ denotes the highest priority. We consider single flow per UE model because, firstly it helps simplify the CBS design by not requiring nested scheduling, ; and secondly, it matches the factory-sensor monitoring scenarios where generally a sensor monitoring a single value is expected. Let Q_u denote the DL queue associated with UE u . Packet arrivals in Q_u follow an *ON/OFF* alternating process with deterministic periods T_{ON}, T_{OFF} . During ON, Poisson arrivals of size S_u bytes arrive at rate λ_{ON} ; none during OFF. The mean rate is $R_u = \frac{\lambda_{ON} S_u T_{ON}}{T_{ON} + T_{OFF}}$, and the aggregate offered load $\Lambda_{DL} \triangleq \sum_{u \in \mathcal{U}} R_u$ defines the normalized load factor $\rho \triangleq \Lambda_{DL} / C_{DL,PHY}$, where $C_{DL,PHY}$ is the cell-edge capacity.

Physical layer abstraction: We fix the numerology $\mu=0$ (15 kHz sub-carrier spacing (SCS)), yielding a slot duration $T_{slot}=1$ ms with $N_{symb}=14$ OFDM symbols² [15]. The system bandwidth B is discretized into N_{RB} resource blocks (RBs) allocated in contiguous resource-block groups (RBGs). Let $n \in \mathbb{N}_0$ denote the discrete slot index, with each slot having a fixed duration T_{slot} . In every slot n , based on CQI, a standard

¹Uplink (UL) is analogous, using Buffer Status Reports (BSRs) for queue state information at the gNB scheduler’s CBS logic.

²Mini-slot scheduling would shorten debit intervals, requiring per-symbol credit updates.

3GPP mapping [16][Table 5.1.3.1-1] selects an MCS index $m_u[n]$ with spectral efficiency and computes the $TBS_u[n]$.

RLC and HARQ configuration: All data bearers operate in radio link control (RLC) unacknowledged mode (UM), avoiding ARQ retransmission delays. RLC acknowledged mode (AM) would further necessitate an extra queue, complicating CBS implementation and adds RLC status PDU delays [17]. Link-layer reliability is provided by HARQ with N_{HARQ} parallel processes; the MAC scheduler always serves pending HARQ retransmissions before new arrivals. Once a PDU is passed from RLC UM to MAC, ownership of the PDU moves to the MAC; any later retransmissions are served from the HARQ buffer within the MAC and never revisit the RLC queue. Therefore, credit is debited only on the *first* grant.

Credit-based shaping: Prior to RA, the gNB applies an IEEE 802.1Qav [5] CBS to each UE queue, with $C_u \in [lo_u, hi_u]$ being the credit of UE u at the start of slot n . The underlying MAC scheduling policy remains unmodified; however, the set of *eligible queues* presented to the scheduler at each TTI is determined by the CBS eligibility criterion. Specifically, only queues with non-negative credit values ($C_u \geq 0$) are considered for RA, creating a credit-gated admission control layer above the standard MAC scheduling logic. While the CBS mechanism can operate with any underlying scheduling algorithm, we implement it with a Round Robin (RR) policy.

IV. DISCRETE-TIME CREDIT-BASED SHAPING FOR 5G NR

We now describe our proposed discrete-time CBS (CBS-DT) mechanism that we have implemented at the gNB MAC layer to provide priority differentiation among UEs. This mechanism adapts concepts from IEEE 802.1Qav to the slotted, resource-block-based structure of the 5G-NR air interface.

A. Per-UE Credit State and Dynamics

For each UE $u \in \mathcal{U}$ with assigned priority $p(u)$, we maintain a state variable $C_u[n]$, called *credit*, representing the accumulated transmission allowance (in Bytes) available at the *beginning* of slot n . This credit value dictates the UE’s eligibility for receiving new transmission grants. The credit evolves from $C_u[n]$ to $C_u[n+1]$ involving a credit *allowance* based on a configured reserved rate (analogous to `idleSlope`) and a credit *debit* $D_u[n]$ based on transmission activity in slot n . Specifically, we define the per-slot credit allowance, ΔC_u (Bytes), derived as $\Delta C_u \triangleq \text{idleSlope}_{p(u)} \cdot T_{slot}$. While continuous-time CBS also incorporates a debit mechanism based on its constant `sendSlope` (as detailed in Eq. (2)), we propose a slot-dependent debit amount $D_u[n]$ (Bytes). Let $X_u[n+1]$ represent the intermediate, unclamped credit calculated at the *end* of slot n (before final clamping), based on the state $C_u[n]$ entering the slot and increments/debits occurring within slot n . The state evolves according to:

$$X_u[n+1] = f(C_u[n], \Delta C_u, Q_u[n]) - D_u[n] \quad (3)$$

where ΔC_u is the per-slot credit allowance (`idleSlope` _{$p(u)$} · T_{slot}), $D_u[n]$ is the debit term (derived later for each CBS variant),

and the function $f(C, \Delta C^{\text{idle}}, Q^{\text{DL}})$ encapsulates the discrete-time adaptation of classical CBS credit accumulation, recovery, and reset rules *prior to debiting*:

$$f(C, \Delta C, Q_u[n]) \triangleq \begin{cases} \min(C + \Delta C, 0) & \text{if } C < 0 \\ 0 & \text{if } C > 0 \wedge Q_u[n] = 0 \\ C + \Delta C & \text{otherwise} \end{cases} \quad (4)$$

Here, $Q_u[n] > 0$ signifies a non-empty buffer for UE u and $D_u[n]$ is the debit term. The final credit state $C_u[n+1]$ is obtained by applying a clamping function $\Gamma(\cdot)$ that enforces the bounds $[lo_u, hi_u]$:

$$C_u[n+1] = \Gamma(X_u[n+1]) \triangleq \min(\max(X_u[n+1], lo_u), hi_u) \quad (5)$$

Note that the $\min(\cdot, lo_u)$ part of $\Gamma(\cdot)$ effectively applies to the output of $f(\cdot)$ before the debit $D_u[n]$ is subtracted in Eq. (3) if we strictly follow the multi-step process; however, for analysis, Eq. (3) and (5) capture the overall state transition. For the CBS-DT adaptation, the debit $D_u[n]$ is coupled to resource granted by the MAC scheduler in slot n . If a new transmission grants yields $TBS_u[n] > 0$ bytes, the debit equals the full grant size:

$$D_u[n] = TBS_u[n] \quad (\text{CBS-DT}) \quad (6)$$

If no new grant is issued, $D_u[n] = 0$. Since the $TBS_u[n]$ varies with channel quality and RA, $D_u[n]$ is inherently a stochastic quantity unlike in CBS.

B. CBS-DT Stability Conditions

The use of a *grant-dependent* debit, $D_u[n]$ (Eq. (6)), introduces stochasticity tied to CQI and RA, departing significantly from the CBS. Nevertheless, the fundamental stability conditions can be established, which are: (i) $C_u[n]$ must remain bounded $\forall n$; (ii) queues must recover from credit deficits. Credit boundedness is directly enforced by the clamping function $\Gamma(\cdot)$ (Eq. (5)) where $C_u[n] \in [lo_u, hi_u]$ for all $n \geq 0$. Deficit recovery (reaching $C_u[n] \geq 0$ from any $C_u[k] < 0$, including the lower bound lo_u) is guaranteed because the per-slot allowance $\Delta C_u > 0$ provides a constant positive increment towards the non-negative region whenever no debit occurs (see Eq. (4)). A comprehensive performance analysis and formal proofs under the full stochasticity introduced by CQI and RA, potentially employing advanced stochastic network calculus, would offer deeper insights but is deferred to future work to maintain focus on the discrete-time adaptation and its fundamental stability properties presented herein.

C. Eligibility Criterion and MAC Interaction

The proposed CBS-DT mechanism shapes traffic by controlling the eligibility of each UE based on accumulated credits. The overall eligibility set $\mathcal{E}[n]$ at slot n is determined by first obtaining the underlying RR MAC scheduler eligibility set $\mathcal{E}_{\text{RR}}[n]$, defined as:

$$\mathcal{E}_{\text{RR}}[n] = \left\{ u \in \{1, \dots, U\}, Q_u[n] > 0, \right. \\ \left. \text{HARQ}_u \text{ available, } u \notin \text{ReTxSet}[n] \right\} \quad (7)$$

Here, HARQ_u available indicates u has free HARQ process and $u \notin \text{ReTxSet}[n]$ ensures that u is not already scheduled

for HARQ retransmission in n . The CBS-DT further restricts eligibility by checking the credit condition:

$$\mathcal{E}[n] = u \in \mathcal{E}_{\text{RR}}[n] | C_u[n] \geq 0 \quad (8)$$

Thus, CBS-DT serves as a credit-based gate layered atop the existing MAC layer.

V. CREDIT-BASED SHAPING WITH PARTIAL USAGE

A key challenge arises with the CBS-DT adaptation due to the practicalities of 5G NR scheduling. While the gNB know the precise downlink queue size, the selected $TBS(n)$ must conform to the quantized values mandated by 3GPP [16]. Consequently whenever the granted $TBS_u[n]$ exceeds $Q_u[n]$, padding is added. CBS-DT, by debiting the *entire* grant $TBS_u[n]$ (Eq. 6), therefore over penalizing the UE. This drives the credit deeper into deficit and postpones the next eligibility event, potentially delaying subsequent transmission eligibility, particularly affecting UEs with bursty arrival traffic patterns. We therefore introduce *Credit-Based Shaping with Partial Usage (CBS-PU)*, that retains the CBS-DT structure outlined in Section IV. The sole modification lies in the definition of the debit term $D_u[n]$ used in the credit.

A. CBS-PU Debit Mechanism

The defining characteristic of CBS-PU is that the credit decrement $D_u[n]$ is proportional to the *actual data transmitted* within the granted resources, rather than the full granted $TBS_u[n]$. The actual bytes for transmission are calculated as:

$$B_u^{\text{actual}}[n] = \min(TBS_u[n], Q_u[n]) \quad (9)$$

Partial Usage Debit: The debit term $D_u[n]$ for the credit update (Eq. (3)) under CBS-PU is equal to:

$$D_u[n] = B_u^{\text{actual}}[n] \quad (\text{CBS-PU}) \quad (10)$$

If no new grant is issued ($TBS_u[n] = 0$), then $B_u^{\text{actual}}[n] = 0$ and thus $D_u[n] = 0$. This ensures credit is consumed only according to the utilized portion of the grant.

B. Theoretical Properties

CBS-PU retains the stability conditions established for the CBS-DT adaptation while offering improved performance characteristics related to credit management.

Theorem 1. *The proposed CBS-PU mechanism ensures:*

- 1) *Credit Dominance:* $C_u^{\text{PU}}[n] \geq C_u^{\text{DT}}[n]$ for all $n \geq 0$, given identical initial conditions and system inputs.
- 2) *Rate Preservation:* For persistently backlogged queues, the long-term average service rate converges to the reserved rate: $\lim_{N \rightarrow \infty} \frac{1}{N} \sum_{n=0}^{N-1} B_u^{\text{actual}}[n] = R_u$.
- 3) *Delay Bound Preservation:* The worst-case delay under CBS-PU is never greater than under CBS-DT: $W_u^{\text{PU}} \leq W_u^{\text{DT}}$.

Proof. (a) Follows by induction on n . Assume $C_u^{\text{PU}}[k] \geq C_u^{\text{DT}}[k]$. Since $f(\cdot)$ and $\Gamma(\cdot)$ are monotonic non-decreasing with respect to credit input, and $D_u^{\text{PU}}[k] = B_u^{\text{actual}}[k] \leq TBS_u[k] =$

$D_u^{DT}[k]$, applying Eqs. (3)-(5) shows $C_u^{PU}[k+1] \geq C_u^{DT}[k+1]$. (b) Let $\alpha_u^+ = \text{idleSlope}_{p(u)}$ be the configured reserved rate. Credit $C_u[n]$ is bounded in $[lo_u, hi_u]$. For a persistently backlogged queue over a long interval N , the total credit change $\sum_{n=0}^{N-1} (\Delta C_u - D_u[n])$ must remain bounded. Thus, $\frac{1}{N} \sum D_u[n] \rightarrow \Delta C_u$. Since $D_u[n] = B_u^{\text{actual}}[n]$ and $\Delta C_u = \alpha_u^+ \cdot T_{\text{slot}}$, the long-term average actual transmitted rate $\frac{1}{NT_{\text{slot}}} \sum B_u^{\text{actual}}[n]$ converges to α_u^+ . (c) Follows directly from credit dominance. Since $C_u^{PU}[n] \geq C_u^{DT}[n]$, a queue cannot become eligible later under CBS-PU than under CBS-DT. Assuming the same MAC scheduling policy for eligible UEs, the departure time under PU must be less than or equal to that under CBS-DT for any given arrival, hence $W_u^{PU} \leq W_u^{DT}$. \square

The primary advantage of CBS-PU arises from property (a). By maintaining higher (or equal) credit levels compared to CBS-DT, especially after partial grant utilization, CBS-PU facilitates faster recovery from credit deficits. This translates to reduced time spent ineligible, potentially lowering queuing delays for bursty traffic, and enables higher resource utilization efficiency (η_u), as empirically validated in Section VI-D.

VI. SIMULATION RESULTS

This section evaluates the performance of the proposed discrete-time CBS adaptations for 5G-NR. Both act as an eligibility-gating (Eq. (8)) layer that selects which UEs are presented to the underlying MAC scheduler. For this study, we employ a RR scheduler. We compare these variants against the RR policy, but considering *all* backlogged UEs without any gating. This allows us to isolate the impact of eligibility gating, demonstrating how it enforces QoS differentiation even when layered atop a non-priority-aware RR allocation mechanism.

A. Simulation Setup

We simulate a single-cell FDD downlink with a 10 Mbps PHY, 15 kHz SCS, and 1 ms slot duration. The radio channel follows the 3GPP UMa model, implemented in our `MyH38901Channel` class; CQI reports are mapped to MCS indices via TS 38.214. All data radio bearers use RLC-UM to avoid multi-queue per-UE complexity and additional status-induced delays in RLC-AM. Six static UEs are divided evenly across three priorities— p_1 (high), p_2 (medium), p_3 (low). Each UE generates traffic as a continuous Poisson process with $\lambda^{\text{ON}}=450$ pkt/s and payload size $S_u=\{80, 160, 240\}$ bytes for p_1, p_2, p_3 , respectively. The aggregate offered rate is $\Lambda_{\text{DL}}=8\lambda^{\text{ON}}\sum_u S_u$, giving a load factor $\rho=\Lambda_{\text{DL}}/C_{\text{DL,PHY}}$; we study $\rho=1$ (nominal) and $\rho=4$ (overload). This overload scenario is useful precisely because it tests the scheduler's behavior under stress and its ability to prioritize and protect high-priority UEs. CBS idle-slope shares are $\{75\%, 20\%, 5\%\}$ for $\{p_1, p_2, p_3\}$ respectively; credit bounds are derived from `maxInterferenceSize=150` Bytes and `maxFrameSize=300` Bytes [5]. The MAC layer employs a RR scheduler from the MATLAB 5G Toolbox's `nrScheduler`. Both CBS-DT and CBS-PU runs on the eligible set $\mathcal{E}[n]$; the RR baseline disables

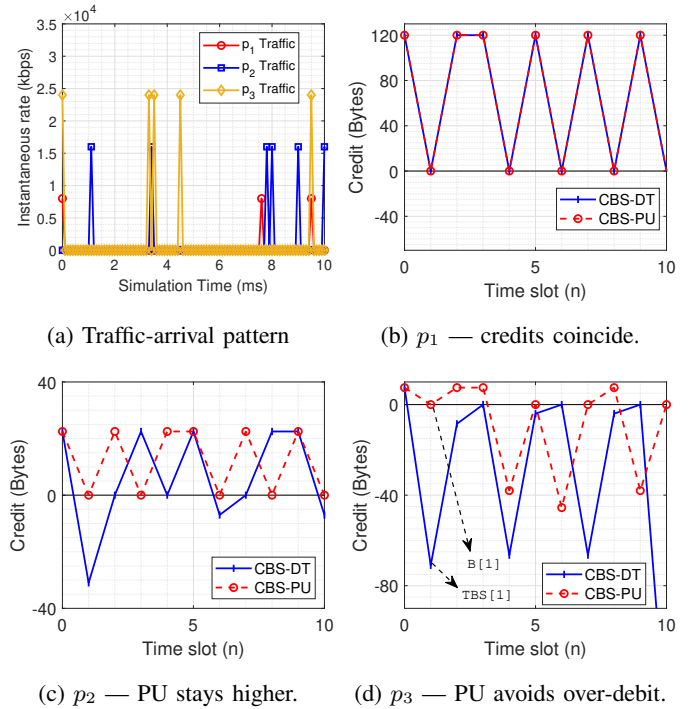


Fig. 3: Overview of traffic arrivals and credit evolution.

credit gating and schedules all back-logged UEs. Custom classes (`MyGNB`, `MyUE`, `MyNetworkTrafficOnOff`, `CBSScheduler`, `CBSSchedulerPartialUsage`) extend the MATLAB 5G-NR Toolbox to track packet latency and per-UE credit, functionality not available in the stock simulator.

B. Credit Evolution Analysis

Fig. 3 depicts representative downlink traffic arrivals (Fig. 3a) with credit ($C_u[n]$) trajectories of one UE per priority class under nominal load for CBS-DT and CBS-PU. High-priority credits, as shown in Fig. 3b, oscillates between 0 and the configured high limit ($hi_u \approx 120$ B) for both variants. The grants are fully utilized, preventing padding. Consequently, the debit terms are identical, resulting in coinciding credit trajectories. In such no-padding conditions, CBS-PU offers no additional benefit over CBS-DT, consistent with Theorem 1(a) where equality holds. Middle-priority UEs (Fig. 3c) show more pronounced credit fluctuations. Under CBS-DT, credits dip moderately into negative territory following transmissions. With CBS-PU, these negative excursions are shallower and recovery is quicker, as the debit accurately reflects smaller actual transmissions ($B_u^{\text{actual}}[n]$) rather than the full $TBS_u[n]$. The largest contrast appears in Fig. 3d). CBS-DT frequently hits the lower credit values requiring lengthy recovery, while CBS-PU significantly mitigates these deficits by debiting only the actual usage. PU yields no change where the queue is always full (p_1), a moderate credit-variance reduction where partial fills are sporadic (p_2), and a drastic reduction where they are frequent (p_3). The plots therefore give a visual, per-priority validation of Theorem 1.

C. Latency Performance Evaluation

We measure end-to-end downlink latency from packet generation at the gNB to successful reception at the UE application layer. Figure 4 presents the empirical CDF by priority under (a) nominal ($\rho = 1.0$), (b) overload ($\rho = 4.0$), comparing RR, CBS-DT, and CBS-PU. At nominal load, as expected, RR shows minimal class isolation, while both CBS variants provide clear latency differentiation favoring p_1 (P99 < 5 ms) over p_2 and p_3 . Notably, CBS-PU yields lower tail latency for p_3 compared to CBS-DT (e.g., 20 ms vs 80 ms 99P), directly reflecting its faster credit recovery mechanism (Fig. 3d). Under overload, RR differentiation collapses entirely. In contrast, both CBS variants robustly protect p_1 latency (99P < 5 ms) while p_3 latency severely degrades (99P \approx 350 ms) due to low reserved bandwidth share for p_3 , with negligible difference between CBS-PU and CBS-DT under such extreme conditions. Thus, CBS provides essential QoS isolation, particularly under congestion, and CBS-PU offers additional latency benefits for lower priorities at moderate loads due to its refined credit accounting.

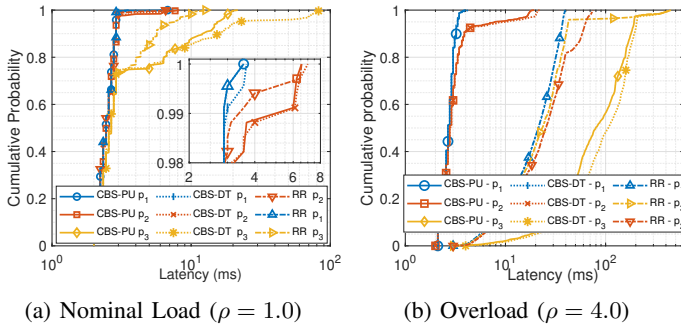


Fig. 4: Empirical CDF of downlink packet latency

D. Resource Utilization Efficiency

We quantify the efficiency of translating granted resources into actual data transmission via $\eta_u = (\sum B_u^{\text{actual}} / \sum \text{TBS}_u) \times 100\%$. Fig. 5 presents η_u evaluated at reduced load ($\rho = 0.2$ Fig. 5a), chosen specifically because partial grant fills ($B_u^{\text{actual}}[n] < \text{TBS}_u[n]$), exposing utilization inefficiencies, that are more prevalent than under high load ($\rho = 0.4$) where buffers are often saturated as shown in Fig. 5b. CBS-PU minimizes *credit waste*, maximizing efficiency (> 98%) by debiting only $B_u^{\text{actual}}[n]$, avoiding penalizing queues for unused grant portions. CBS-DT suffers efficiency loss from TBS debiting. Its $\text{TBS}_u[n]$ debit creates *credit waste* when $B_u^{\text{actual}}[n] < \text{TBS}_u[n]$. This not only reduces the η_u ratio directly but also prolongs credit recovery, hence increasing the latency as observed in Section VI-C. The resulting efficiency ($\approx 95\text{--}98\%$) reflects this penalty. RR's policy, despite using buffer information, results in frequent resource mismatches where $B_u^{\text{actual}}[n] \ll \text{TBS}_u[n]$, yielding the lowest efficiency ($\approx 80\text{--}85\%$ for p_3).

VII. CONCLUSION

This paper presented and evaluated two discrete-time adaptations of CBS with 5G-NR RAN: CBS-DT using granted TBS

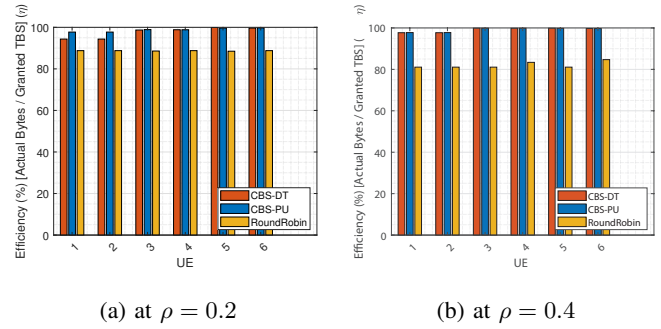


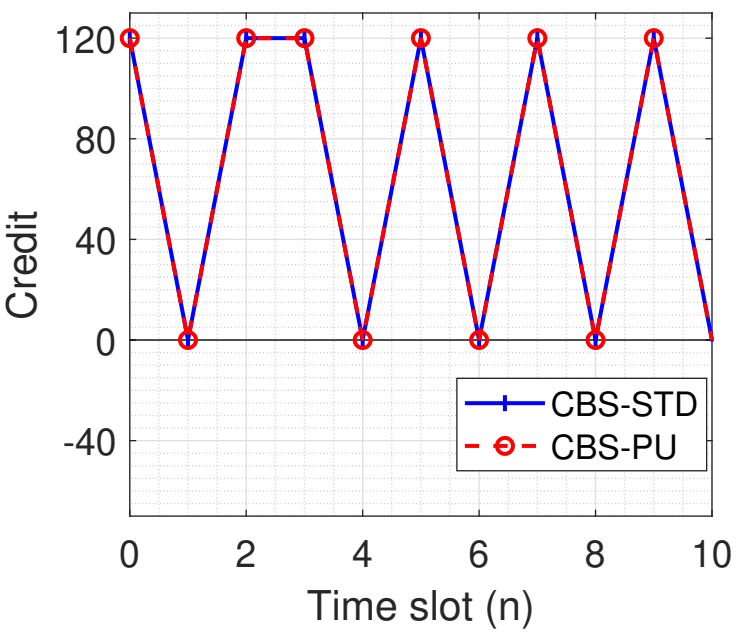
Fig. 5: Per-UE downlink resource utilization efficiency (η_u) comparison at reduced load.

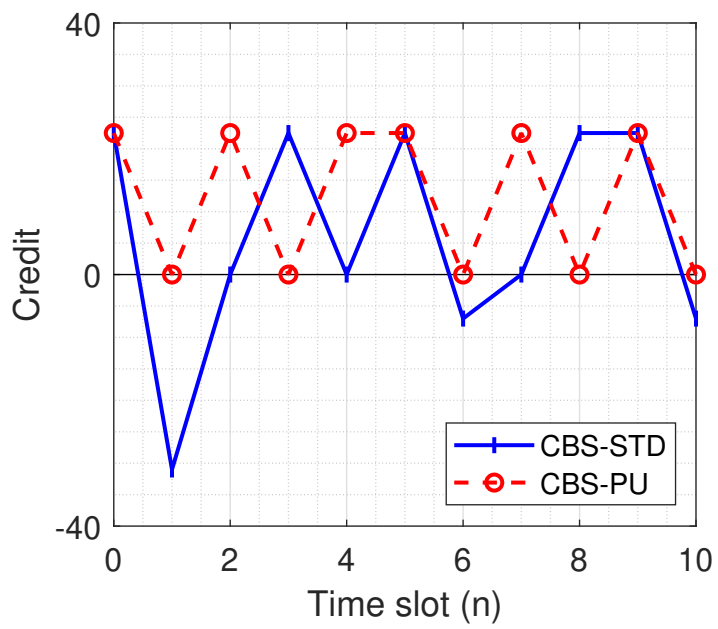
for debiting and CBS-PU debiting based on estimated actual transmitted bytes. Through MATLAB 5G Toolbox simulations comparing these variants against RR, we demonstrated that both CBS mechanisms successfully enforce strict priority-based latency differentiation atop a non-QoS scheduler like RR, especially under heavy load. Critically, we observe that CBS-DT is inefficient due to full TBS debiting, and proposed CBS-PU to avoid excessive credit deficits when grants are partially utilized. This resulted in faster credit recovery for lower-priority UEs and superior resource utilization efficiency while preserving the essential QoS guarantees of CBS. Our findings indicate that CBS-PU offers a promising approach for achieving both deterministic performance and high resource utilization efficiency in 5G/6G systems supporting time-sensitive applications.

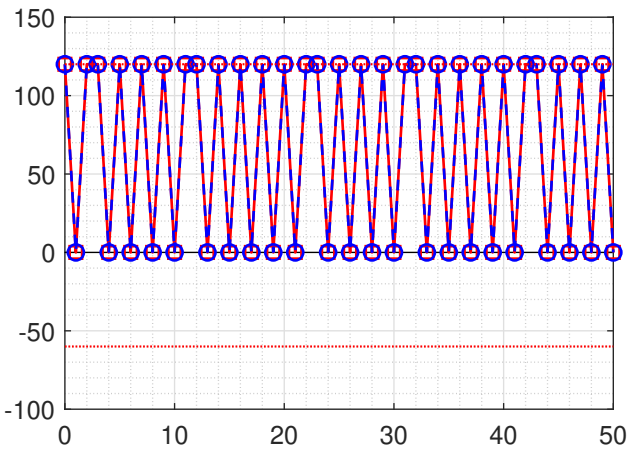
REFERENCES

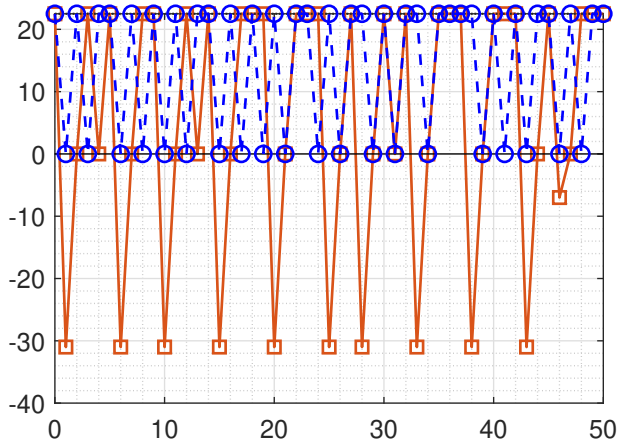
- [1] W. Saad, M. Bennis, and M. Chen, "A vision of 6g wireless systems: Applications, trends, technologies, and open research problems," *IEEE Network*, vol. 34, no. 3, pp. 134–142, 2020.
- [2] W. Xiang *et al.*, "Advanced Manufacturing in Industry 5.0: A Survey of Key Enabling Technologies and Future Trends," *IEEE Transactions on Industrial Informatics*, vol. 20, no. 2, pp. 1055–1068, 2024.
- [3] J. Sasiain *et al.*, "Toward the Integration and Convergence Between 5G and TSN Technologies and Architectures for Industrial Communications: A Survey," *IEEE Communications Surveys & Tutorials*, vol. 27, no. 1, pp. 259–321, 2025.
- [4] G. P. Sharma *et al.*, "Toward Deterministic Communications in 6G Networks: State of the Art, Open Challenges and the Way Forward," *IEEE Access*, vol. 11, pp. 106 898–106 923, 2023.
- [5] "IEEE standard for local and metropolitan area networks— virtual bridged local area networks amendment 12: Forwarding and queuing enhancements for time-sensitive streams," *IEEE Std 802.1Qav-2009 (Amendment to IEEE Std 802.1Q-2005)*, pp. 1–72, 2010.
- [6] J. John *et al.*, "Industry 4.0 and Beyond: The Role of 5G, Wi-Fi 7, and Time-Sensitive Networking (TSN) in Enabling Smart Manufacturing," *Future Internet*, vol. 16, no. 9, 2024. [Online]. Available: <https://www.mdpi.com/1999-5903/16/9/345>
- [7] K. Kosek-Szott, M. Natkaniec, and L. Prasnal, "IEEE 802.11aa intra-AC prioritization - A new method of increasing the granularity of traffic prioritization in WLANs," in *2014 IEEE Symposium on Computers and Communications (ISCC)*, 2014, pp. 1–6.
- [8] K. Nihileswar, K. Prabhu, D. Cavalcanti, and A. Regev, "Time-sensitive networking over 5g for industrial control systems," in *2022 IEEE 27th International Conference on Emerging Technologies and Factory Automation (ETFA)*, 2022, pp. 1–8.
- [9] Y. Zhang *et al.*, "QoS-Aware Mapping and Scheduling for Virtual Network Functions in Industrial 5G-TSN Network," in *2021 IEEE Global Communications Conference (GLOBECOM)*, 2021, pp. 1–6.
- [10] M. K. Atiq *et al.*, "When IEEE 802.11 and 5G Meet Time-Sensitive Networking," *IEEE Open Journal of the Industrial Electronics Society*, vol. 3, pp. 14–36, 2022.

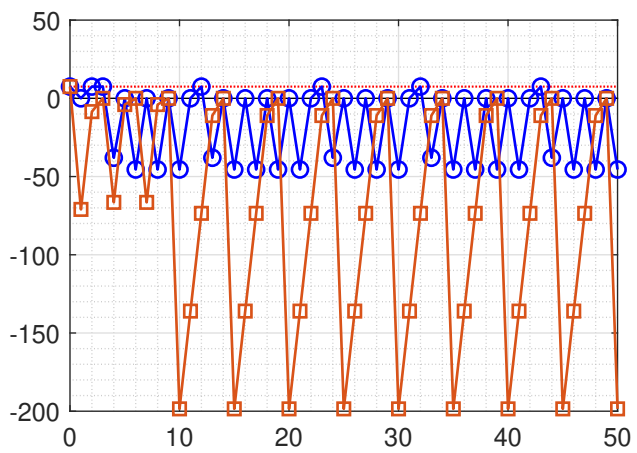
- [11] Z. Satka, D. Pantzar, A. Magnusson, M. Ashjaei, H. Fotouhi, M. Sjödin, M. Daneshlab, and S. Mubeen, "Developing a Translation Technique for Converged TSN-5G Communication," in *2022 IEEE 18th International Conference on Factory Communication Systems (WFCS)*, 2022, pp. 1–8.
- [12] H. Hassani, P. J. L. Cuijpers, and R. J. Bril, "Work-in-Progress: Layering Concerns for the Analysis of Credit-Based Shaping in IEEE 802.1 TSN," in *2020 16th IEEE International Conference on Factory Communication Systems (WFCS)*, 2020, pp. 1–4.
- [13] J. Cao, "An Independent Timing Analysis for Credit-Based Shaping in Ethernet TSN," Phd Thesis 1 (Research TU/e / Graduation TU/e), Mathematics and Computer Science, Jun. 2023, proefschrift.
- [14] K. Haneda *et al.*, "5G 3GPP-Like Channel Models for Outdoor Urban Microcellular and Macrocellular Environments," in *2016 IEEE 83rd Vehicular Technology Conference (VTC Spring)*, 2016, pp. 1–7.
- [15] H. Tataria *et al.*, "6G Wireless Systems: Vision, Requirements, Challenges, Insights, and Opportunities," *Proceedings of the IEEE*, vol. 109, no. 7, pp. 1166–1199, 2021.
- [16] 3GPP, "Technical Specification Group Radio Access Network; NR; Physical layer procedures for data," 3rd Generation Partnership Project (3GPP), 3GPP TS 38.214 V16.2.0, Oct. 2020, Release 16. [Online]. Available: https://www.3gpp.org/ftp/Specs/archive/38_series/38.214/
- [17] M. Irazabal, E. Lopez-Aguilera, I. Demirkol, R. Schmidt, and N. Nikaein, "Preventing RLC Buffer Sojourn Delays in 5G," *IEEE Access*, vol. 9, pp. 39 466–39 488, 2021.

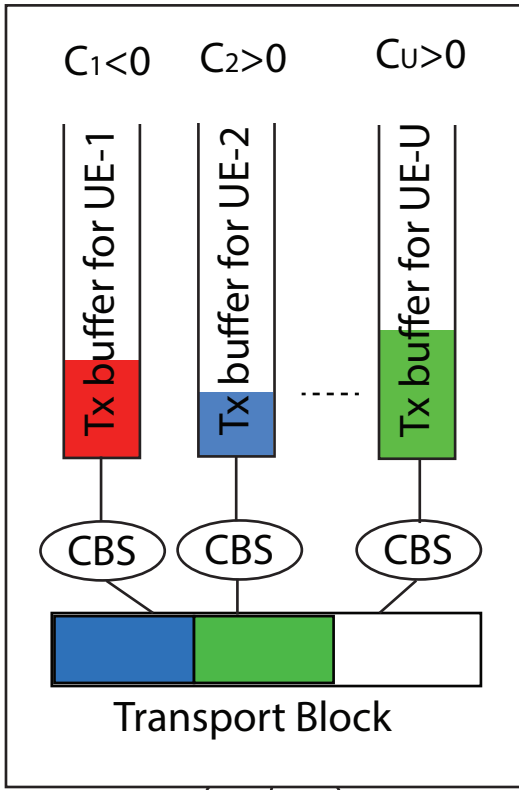






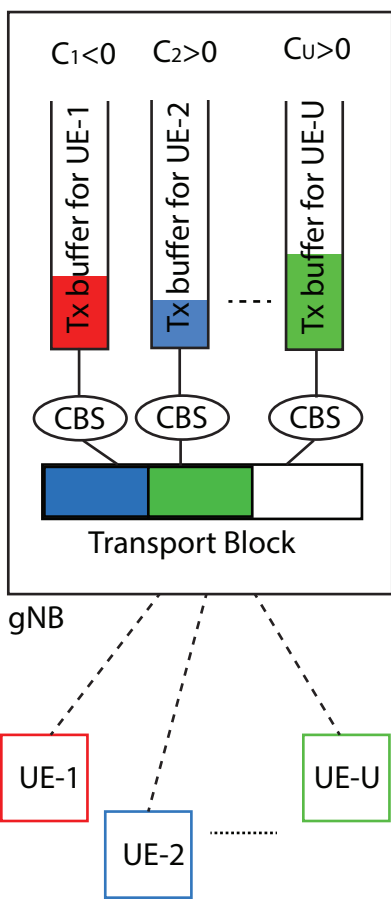


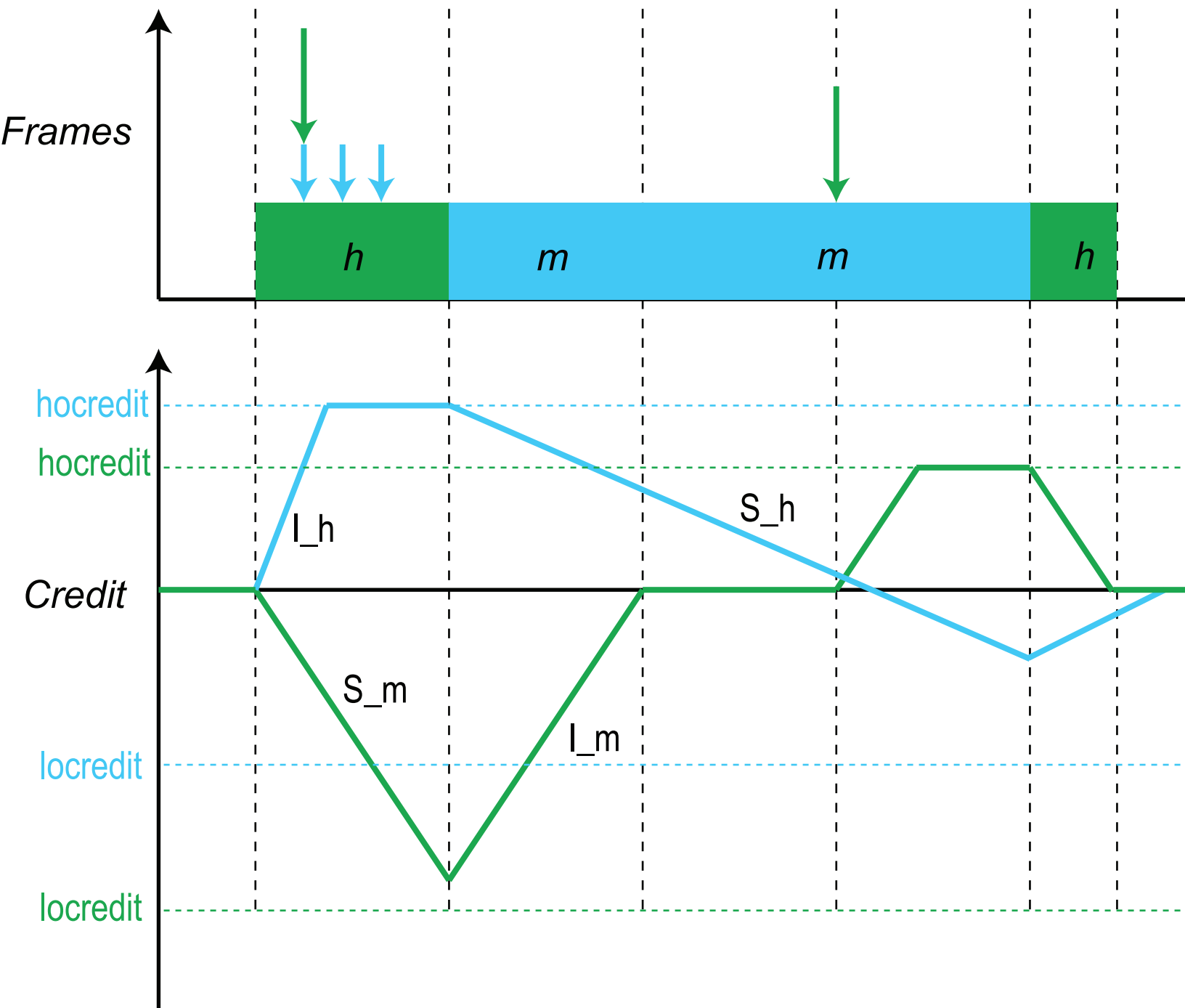




gNB



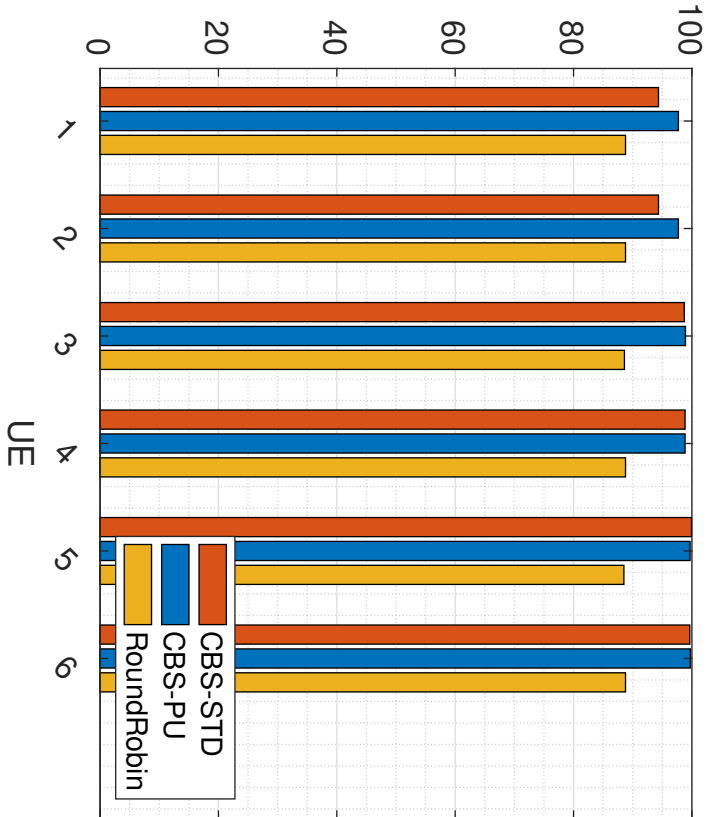




This figure "fig1.png" is available in "png" format from:

<http://arxiv.org/ps/2505.12091v1>

Efficiency (%) [Actual Bytes / Granted TBS] (η)



Efficiency (%) [Actual Bytes / Granted TBS] (η)

